Molecular Phylogenetics and Evolution 98 (2016) 74–83

Contents lists available at ScienceDirect

Molecular Phylogenetics and Evolution

journal homepage: www.elsevier.com/locate/ympev

Mitochondrial comparative genomics and phylogenetic signal assessment of mtDNA among arbuscular mycorrhizal fungi ☆

Maryam Nadimi, Laurence Daubois, Mohamed Hijri *

Institut de Recherche en Biologie Végétale, Département de Sciences Biologiques, Université de Montréal, 4101 Rue Sherbrooke Est, Montréal (Québec) H1X 2B2, Canada

ARTICLE INFO

Article history:
Received 21 January 2015
Revised 16 December 2015
Accepted 14 January 2016
Available online 8 February 2016

Keywords:
Arbuscular mycorrhizal fungi
Fungi
Comparative mitochondrial genomics
Genome evolution
Phylogenetic analysis

ABSTRACT

Mitochondrial (mt) genes, such as cytochrome C oxidase genes (*cox*), have been widely used for barcoding in many groups of organisms, although this approach has been less powerful in the fungal kingdom due to the rapid evolution of their mt genomes. The use of mt genes in phylogenetic studies of Dikarya has been met with success, while early diverging fungal lineages remain less studied, particularly the arbuscular mycorrhizal fungi (AMF). Advances in next-generation sequencing have substantially increased the number of publically available mtDNA sequences for the Glomeromycota. As a result, comparison of mtDNA across key AMF taxa can now be applied to assess the phylogenetic signal of individual mt coding genes, as well as concatenated subsets of coding genes. Here we show comparative analyses of publically available mt genomes of Glomeromycota, augmented with two mtDNA genomes that were newly sequenced for this study (*Rhizophagus irregularis* DAOM240159 and *Glomus aggregatum* DAOM240163), resulting in 16 complete mtDNA datasets. *R. irregularis* isolate DAOM240159 and *G. aggregatum* isolate DAOM240163 showed mt genomes measuring 72,293 bp and 69,505 bp with G + C contents of 37.1% and 37.3%, respectively. We assessed the phylogenies inferred from single mt genes and complete sets of coding genes, which are referred to as "supergenes" (16 concatenated coding genes), using Shimodaira–Hasegawa tests, in order to identify genes that best described AMF phylogeny. We found that *rnl*, *nad5*, *cox1*, and *nad2* genes, as well as concatenated subset of these genes, provided phylogenies that were similar to the supergene set. This mitochondrial genomic analysis was also combined with principal coordinates and partitioning analyses, which helped to unravel certain evolutionary relationships in the *Rhizophagus* genus and for *G. aggregatum* within the Glomeromycota. We showed evidence to support the position of *G. aggregatum* within the *R. irregularis* 'species complex'.

1. Introduction

Elucidating the population structure and inferring the evolutionary histories of species are critical toward understanding their role in ecosystems, and for microorganisms, this generally requires a molecular approach. Developing effective methods, genetic markers, and discriminating criteria are key to phylogenetic analysis and species diagnosis. Mitochondrial (mt) genes and genomes have been used extensively in phylogenetic and population genetic studies of a wide range of organisms. Typical mt genomes comprise a single molecule of DNA, which is usually circular and contains all mt genes, while the number of mt genes varies among species. It has often been assumed that the phylogenetic signal of each mt gene is identical, or highly similar, due to the physical proximity of these genes which lie within the same mtDNA molecule (Avise, 1994). However, mtDNA analyses in many organisms have suggested divergence in the phylogenetic signal strength of mt genes among and within species (Duchene et al., 2011). Several studies have indicated that sequencing of complete mtDNA molecules, referred to as "supergenes" (i.e. complete set of mt protein coding genes), provides the highest phylogenetic resolution among studied animals (Duchene et al., 2011; Fenn et al., 2008; Havird and Santos, 2014). In addition, recent developments in next-generation sequencing technologies have generated a huge number of mtDNA datasets across a broad range of organisms, in particular in the kingdom Animalia (Duchene et al., 2011; Havird and Santos, 2014). These publically available mtDNA datasets offer opportunities to perform large-scale comparative mt genomic analyses, to infer phylogenetic relationships (for identification purposes) and to compare the phylogenetic signals of complete sets of mt genes, or of concatenated subsets of individual mt genes. Numerous phylogenetic studies have been performed on single mt genes such

☆ This paper was edited by the Associate Editor J.-M. Moncalvo.

* Corresponding author.
E-mail address: Mohamed.Hijri@umontreal.ca (M. Hijri).

http://dx.doi.org/10.1016/j.ympev.2016.01.009
1055-7903/

as cytochrome C oxidase subunit 1 (*cox1*) (Borriello et al., 2014; Hebert et al., 2003; Ratnasingham and Hebert, 2007; Roe and Sperling, 2007) and the mitochondrial large subunit gene (*rnl*) to infer evolutionary relationships between organisms (Borstler et al., 2008; Bruns et al., 1998). However, the phylogenetic signals produced by these extensively studied genes have not often been compared with the complete set of mt genes or with other mt gene subsets. Such comparative analyses are key to accurately assessing the evolutionary relationships of mt genomes within a given group of organisms, and for identifying genes with strong phylogenetic signals that can be used to discriminate between closely related taxa. For instance, the arbuscular mycorrhizal fungi (AMF), a group of closely related symbionts of plant roots, are notoriously difficult to characterize and distinguish through molecular methods. A more comprehensive mitochondrial-based approach could provide a solution to this issue.

The arbuscular mycorrhizal fungi are obligate biotrophs among the most abundant eukaryotic symbionts of plants, and not only improve plant mineral uptake and enhance plant productivity and diversity (Smith and Read, 2008), but also help in the control of plant pathogens (Azcón-Aguilar and Barea, 1997; Garcia-Garrido and Ocampo, 2002; Ismail and Hijri, 2012; Ismail et al., 2011) and stimulate the fitness of plants in polluted environments (Hildebrandt et al., 1999; Zhang et al., 2014). The AMF constitute an early diverging fungal lineage, whose mycelia are typically formed by coenocytic branching hyphae (i.e. hyphae that lack septae) in which nuclei and cell organelles including mitochondria can freely move through the hyphal network (Marleau et al., 2011). Mitochondria inheritance in Glomeromycota as well as in fungi has been discussed in Nadimi et al. (2015). In addition AMF interact closely with bacteria and fungi that were found inside their mycelia as well as adhering on the surface of spores and hyphae where the form biofilm-like structures (Hijri et al., 2002; Bianciotto et al., 2003; Scheublin et al., 2010; Lecomte et al., 2011; Iffis et al., 2014). Although, AMF have been shown to harbor a complete and functional meiotic and pheromone-sensing pathway, as well as sets of mating types (Halary et al., 2013, 2011; Pelin et al., 2012), sexual reproduction has not yet been observed. Limitations in distinguishing morphological characters and molecular traits are among the major factors limiting progress in AMF research. In addition, intra-isolate genetic polymorphism and nuclear organization are still under debate. Some studies referred to AMF as monokaryotic organisms (Pawlowska and Taylor, 2004; Tisserant et al., 2013; Ropars and Corradi, 2015), while many lines of evidence supported the theory that AMF harbor genetically different nuclei in a common cytoplasm, making these organisms highly unusual (Angelard et al., 2010; Beaudet et al., 2015; Boon et al., 2015, 2010, 2013; Hijri and Sanders, 2005; Kuhn et al., 2001). Initial species definition of the Glomeromycota was based on the morphology of spores and spore clusters such as spore wall ontogeny, size, shape, color, hyphal attachment and reaction to staining solutions (e.g. Melzer's). Currently, molecular phylogeny based on the analysis ribosomal rDNA sequences combined with morphology, are used for species definition in Glomeromycota (Schüssler and Walker, 2010). In contrast to the nuclear genomes of AMF, mitochondrial coding-genes such as *rnl* and *cox1*, as well as complete mtDNAs, have been reported to be homogeneous in many AMF taxa (Borstler et al., 2008; Lee and Young, 2009; Raab et al., 2005; Thiery et al., 2010), although this has been challenged by Beaudet et al. (2015). Investigating large datasets of mtDNAs could offer opportunities to advance our understanding of the population genomics and phylogeny of AMF.

To date, 16 fully sequenced Glomeromycota mt genomes have been published, representing two major glomeromycotan families: the Glomeomeraceae (14 mtDNAs) and the Gigasporaceae (two mtDNAs) (Beaudet et al., 2013a, 2013b; de la Providencia et al., 2013; Formey et al., 2012; Nadimi et al., 2012, 2015; Pelin et al., 2012). These mtDNA datasets offer opportunities to compare the intra- and inter-specific diversity of mt genomes and genes among closely related AMF taxa, as well as the usefulness of various mt genes in phylogenetic analyses. In this study, we sequenced and mapped the mtDNAs of two AMF species, *Rhizophagus irregularis* DAOM240159 and *Glomus aggregatum* DAOM240163, to augment the publically available set of AMF mtDNAs. We performed a mitogenomics comparative analysis, as well as principal coordinate and partitioning analyses, in order to: (1) assess the phylogenetic signals of mt coding genes; (2) evaluate their potential use in inferring AMF phylogenies; and (3) unravel evolutionary relationships within the *Rhizophagus* genus.

2. Materials and methods

2.1. Fungal material and DNA extraction

Spores and mycelium of a *Glomus aggregatum* isolate (DAOM240163) and of a *Rhizophagus irregularis* isolate (DAOM240159) were cultivated *in vitro* on a minimal (M) medium with carrot roots that had been transformed with *Agrobacterium rhizogenes* (Bécard and Fortin, 1988). The medium was dissolved using a solution of 0.82 mM sodium citrate and 0.18 mM citric acid, and fungal mycelia were collected by sieving the suspension. The collected fungal material was checked for root contamination under a binocular microscope. DNA extraction was performed using the DNeasy Plant kit (Qiagen, Mississauga, ON) according to the manufacturer's instructions.

2.2. Sequencing, assembly and gene annotation

Whole genome shotgun sequencing was performed using Roche 454 GS FLX Titanium technology, with one full run per isolate. Sequencing was performed at the Genome Quebec Innovation Center (McGill University, Montreal, QC). The reads were *de novo* assembled with Newbler v2.9 at the Genome Quebec facility, and mitochondrial contigs were identified and pooled for each isolate. Gene annotation was performed using an automated mt annotator MFannot (http://megasun.bch.umontreal.ca/cgi-bin/mfannot/mfannotInterface.pl), followed by manual inspection. The *R. irregularis* DAOM197198 mtDNA (accession number HQ189519) was used as reference for sequence analyses and mtDNA comparison. Sequencing of the PCR products (acquired for joining mtDNA contigs) was performed using Sanger technology at the Genome Quebec Innovation Center (McGill University, Montreal, Canada). The annotated mtDNAs of *R. irregularis* DAOM240159 and *G. aggregatum* DAOM240163 were deposited in GenBank under the accession numbers KM586389 and KM586390, and circular maps were built using OGDraw v. 1.2 software (Lohse et al., 2013). Comparative sequence analyses were performed using the National Center for Biotechnology Information (NCBI) genomic database and multiple sequence alignment. Nucleotide blast was used for similarity analyses, followed by amino acid comparisons for more distinct sequences. A search with tBLASTX was also performed using a minimum *E*-value cutoff of 1e−10 and 50% minimum identity.

2.3. Polymerase chain reactions (PCR)

As mentioned above, conventional PCRs were used to fill the gaps between mt contigs in order to complete the mtDNA genome for each isolate. Conventional PCRs were performed in a final volume of 50 µl containing 1× PCR buffer, 1.5 mM $MgCl_2$, 0.2 mM of each deoxynucleotide triphosphate (dNTP), 0.5 µM of

each primer, 1 unit of Platinum *Taq* DNA Polymerase (Life Technologies, Burlington, ON), and 5–20 ng of genomic DNA was used as a template. Cycling parameters were: 94 °C for 90 s, followed by 38 cycles of 94 °C for 1 min, annealing temperature (variable based on the designed primers but generally ~60 °C) for 30 s, 72 °C for 90 s and a final elongation at 72 °C for 5 min. PCR products were directly sequencing as described above.

2.4. Datasets and sequence alignments

Sixteen completely sequenced mt-genomes whose length ranged between 59,633 bp (*G. cerebriforme*) and 97,349 bp (*Gigaspora rosea*) were used in comparative analyses. The complete mtDNA alignment was evaluated for phylogenetic and comparative mitogenomic analyses. 16 genes containing 14 protein-coding genes (*atp6*, *atp8*, *atp9*, *cox1*, *cox2*, *cox3*, *nad1*, *nad2*, *nad3*, *nad4*, *nad4L*, *nad5*, *nad6* and *cob*) and two ribosomal coding subunits (*rns* and *rnl*) were concatenated to construct the "supergene" set. Multiple nucleotide sequence alignment was performed using ClustalW as implemented in MUSCLE version 3.8.31 (Edgar, 2004). The number and percentage of polymorphic sites per gene, sequence length and overall average of mean distance of the 16 mitochondrial genes used in the study, are summarized in Table 1. Polymorphic sites were computed using DnaSP v5 (Librado and Rozas, 2009).

2.5. Phylogenetic analyses

Phylogenetic analyses were performed for all mt genes from fully sequenced mtDNAs of AMF isolates (Table 2). Nucleotide alignments of all datasets were used to infer maximum likelihood (ML) phylogenies as implemented in RAxML (Stamatakis et al., 2008), using the RAxML-HPC2 on XSEDE web-server at CIPRES [http://www.phylo.org] (Miller et al., 2010). Node support was determined using rapid bootstrapping with 1000 replicates. All datasets were analyzed using the GTRGAMMA model. Phylogenies were also generated for the datasets using concatenation of all mt genes (supergene set) and for a subset of genes, using concatenation of the four best-performing mt genes (genes that showed similar tree topology to that of supergene).

Table 1
Polymorphic sites and the overall average of mean distance of 16 mitochondrial genes used in the study.

Genes	Overall average of mean distance	Length (bp)	Number of polymorphic sites	Percentage of polymorphic sites (%)
rnl	131.9	2965	536	18.1
nad5	158.1	2478	707	28.5
cox1	107.8	1586	436	27.5
nad2	138.8	1554	553	35.6
rns	195.4	1512	802	53.0
nad4	30.2	1500	134	8.9
nad3	47.7	1242	174	14.0
cob	97	1157	386	33.4
nad1	86.2	975	359	36.8
cox2	67.9	852	270	31.7
atp6	102	816	359	44.0
cox3	63.4	809	259	32.0
nad6	48.3	579	200	34.5
nad4L	51.6	276	216	78.3
atp9	16.8	225	65	28.9
atp8	13.8	147	59	40.1

Table 2
Arbuscular mycorrhizal fungal isolates used in our mitogenomic analyses. PCGs means protein coding genes; NM means not mentioned.

Species	Isolates	Cultures	Accession	Length (pb)	PCGs	rRNAs	tRNAs	SIRs	Number of introns in PCGs				References
									Number of *dpos*	*nad5*	*cox1*	*cox3*	*cob*	
Rhizophagus irregularis	494	*In vitro*	FJ648425	70,606	14	2	26	NM	NM	2	11	3	4	Lee and Young (2009)
Rhizophagus irregularis	DAOM197198	*In vitro*	HQ189519	70,800	14	2	25	NM	NM	2	11	3	4	Nadimi et al. (2012)
Rhizophagus irregularis	DAOM234179	*In vitro*	KC164354	75,075	14	2	25	31	10	2	11	3	4	Beaudet et al. (2013b)
Rhizophagus irregularis	DAOM240415	*In vitro*	JX993113	70,781	14	2	25	NM	8	2	11	3	4	de la Providencia et al. (2013)
Rhizophagus irregularis	DAOM234328	*In vitro*	JX993114	68,994	14	2	25	NM	8	2	11	3	4	de la Providencia et al. (2013)
Rhizophagus irregularis	MUCL46239	*In vitro*	JQ514223	87,755	14	2	25	NM	NM	2	12	3	NM	Formey et al. (2012)
Rhizophagus irregularis	MUCL46240	*In vitro*	JQ514225	74,798	14	2	25	NM	NM	2	9	3	NM	Formey et al. (2012)
Rhizophagus irregularis	MUCL43204	*In vitro*	JQ514224	87,755	14	2	25	NM	NM	2	12	3	NM	Formey et al. (2012)
Rhizophagus sp.	DAOM229456	*In vitro*	JX065416	87,763	14	2	25	NM	2	2	14	3	5	Beaudet et al. (2013a)
Rhizophagus sp.	DAOM240422	*In vitro*	KC164355	86,170	14	2	25	29	10	2	11	3	4	Beaudet et al. (2013b)
Rhizophagus sp.	DAOM213198	*In vitro*	KF591215/6	91,020	14	2	25	20	11	3	13	3	7	Nadimi et al. (2015)
Rhizophagus irregularis	DAOM240159	*In vitro*	KM586389	72,293	14	2	25	2	9	2	10	3	4	This study
Glomus aggregatum	DAOM240163	*In vitro*	KM586390	69,505	14	2	25	33	7	2	9	3	4	This study
Glomus cerebriforme	DAOM227022	*In vitro*	KC164356	59,633	14	2	25	40	2	1	5	2	2	Beaudet et al. (2013b)
Gigaspora rosea	DAOM194757	*In vivo*	NC_016985	97,350	14	2	25	NM	2	3	10	–	1	Nadimi et al. (2012)
Gigaspora margarita	BEG34	*In vivo*	NC_016684	96,998	14	2	25	NM	NM	3	7	1	1	Pelin et al. (2012)

2.6. Statistical analysis of phylogenies

Topologies of each dataset, composed of each of the 16 mt genes, or a subset of the four best-performing mt genes with different combinations were compared to the supergene set. Statistical analyses of the comparisons of phylogenetic signals for different datasets, as well as comparisons of the topologies derived from mt genes and that of supergene, were performed using Shimodaira–Hasegawa (SH) tests, implemented in RAxML using '-f h' parameters locally. The SH test provides log-likelihood values and the variation scores (Ln *L*) between the supergene topology and each of the topologies inferred from single mt gene subsets, with respect to the standard deviation (SD). This test was performed for phylogenies inferred using the ML approach based on nucleotide datasets.

2.7. Distance matrix, principal coordinate analysis, and partitioning analysis

All analyses were conducted in R v.3.0.2 (R Foundation for Statistical Computing; available at http://www.R-project.org). Using the 'read.alignment' function of the 'seqinr' packages (Charif and Lobry, 2007), 'dist.hamming', 'dist.dna' and 'dist.ml' of the 'phangorn' package (Paradis et al., 2004) distance matrices were computed from nucleotide concatenated alignment of the 16 genes used in this study. The similarity relationship between isolates was assessed with a principal coordinate analysis (PCoA) plot, using the 'pcoa' function of the 'ape' package (Paradis et al., 2004). In order to detect isolate clusters within the plot, partitioning analysis were computed using a K-means clustering approach, and analyses were computed using 'kmeans' of the 'fpc' package (Hennig, 2010), looking for a bend in the sum of squared roots (SSE). We also used partitioning around k-medoids to estimate the number of clusters, using the 'pamk' function of the 'fpc' package (Hennig, 2010).

3. Results and discussion

3.1. Overview of mtDNA diversity and evolution in the Glomeromycota

Fourteen complete mtDNAs belonging to two orders (Glomerales and Diversisporales) and three genera (*Glomus*, *Rhizophagus* and *Gigaspora*) were retrieved from public databases, and this dataset was augmented by two newly sequenced mtDNAs, resulting in a total of 16 mtDNAs from the Glomeromycota phylum (Table 2). Although mt genome structure and genome synteny varies somewhat among the studied isolates, they all contain 14 protein-coding genes and 2 ribosomal subunit genes. *R. irregularis* isolate DAOM240159 and *G. aggregatum* isolate DAOM240163 are the two newly sequenced mt genomes, measuring 72,293 bp and 69,505 bp, with G + C contents of 37.1% and 37.3%, respectively (Fig. 1). Both mitochondrial genomes harbor the full set of typical fungal genes, such as three subunits of ATP synthase (*atp6*, *atp8* and *atp9*), three cytochrome oxidase subunits (*cox1*, *cox2* and *cox3*), seven subunits of the NADH dehydrogenase (*nad1*, *nad2*, *nad3*, *nad4*, *nad5*, *nad6* and *nad4L*) and apocytochrome b (*cob*). They encode 25 tRNAs and small and large ribosomal subunits (mtSSU and mtLSU) (Fig. 1). In total, 41 genes encoded on the same strand in both genomes are found in each mtDNA (Fig. 1). The annotated sequences of *R. irregularis* DAOM240159 and *G. aggregatum* DAOM240163 were deposited in GenBank under the accession numbers KM586389 and KM586390, respectively. Our phylogenetic analysis, based on the concatenation of all individual mt genes (supergene), clustered *G. aggregatum* within the *R. irregularis* group. However, using sequence comparison of intergenic regions, we were able to discriminate *G. aggregatum* and *R. irregularis* isolates (Table 3). *G. aggregatum* was described by Schenck and Smith in 1982 after being found in the roots of citrus trees in Florida (Schenck and Smith, 1982). Spores can be formed individually in the soil and in roots or aggregates without a peridium. These spores are globose, subglobose, obovate, and cylindrical to irregular. In fact, *G. aggregatum* and *R. irregularis* are very close according

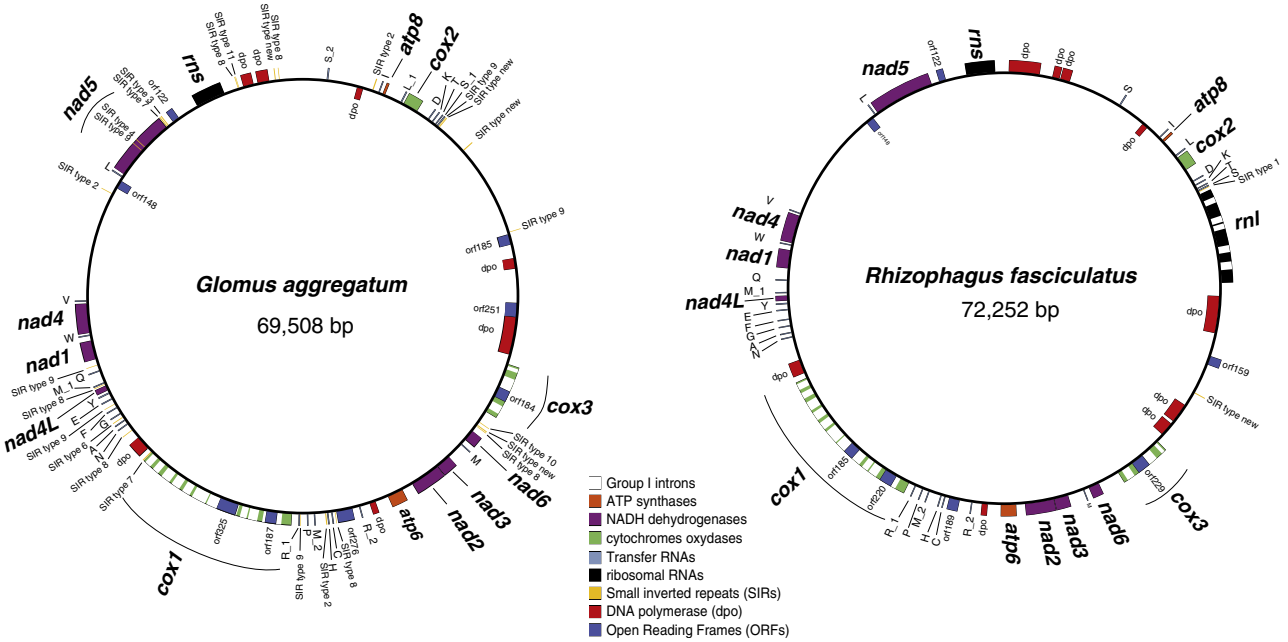

Fig. 1. Comparison of the mitogenomes of the *Glomus aggregatum* isolate (DAOM240163) and the *Rhizophagus irregularis* isolate (DAOM240159). The circular mapping genomes were opened upstream of *rnl*. Genes on the outer and inner circumference are transcribed in a clockwise and counterclockwise direction, respectively. Gene and corresponding product names are *cox1–3*, cytochrome c oxidase subunits, *atp6*, *8*, *9*, ATP synthase subunits; cob, apocytochrome b; *nad1–4*, *4L*, *5–6*, NADH dehydrogenase subunits; *rnl*, *rns*, large and small subunit rRNAs; A–W, tRNAs, the letter corresponding to the amino acid specified by the particular tRNA followed by their anticodon.

Table 3
Sequence comparison of intergenic regions between *R. irregularis* 197198 and *G aggregatum*.

IGRs	Variable regions position
rnl-cox2	41 bp insertion in position 1042 in *G. aggregatum*
nad3-nad6	37 bp insertion in position 88 in *G. aggregatum*
nad5-cob	40 bp insertion in position 927 in *G. aggregatum*
nad4L-cox1	Polymorphism from 748 to 787 bp in DAOM197198 and 745–795 in *G. aggregatum*
atp9-rns	65 bp deletion from position 5550 in *G. aggregatum*
	Polymorphism from 5410 to 5424 bp in DAOM197198 and 745–795 in *G. aggregatum*
nad6-cox3	36 bp insertion in position 557 in *G. aggregatum*
cox3-rnl	8628 bp insertion in position 1 in *G. aggregatum*
	About 7500 bp polymorphism at position 404 of DAOM197198 (9034 in *G. aggregatum*)

to the morphological characters of their sp[illegible], with the only tar[illegible] difference being that *G. aggregatum* spores possess an inner laminated wall that strongly reacts to Melzer's reagent, while the inside of spores are sometimes differentiated (Sokolski et al., 2011). A phosphate transporter gene was able to slightly discriminate *G. aggregatum* from a dozen *R. irregularis* isolates (Sokolski et al., 2011), while other genes such as ATPase H+, ATPaseF0F1, as well as ITS, 18R and 25S rRNA genes were not able to discriminate these two species. In a recent reclassification of the Glomeromycota, the position of *G. aggregatum* was classified as uncertain (Schüssler and Walker, 2010).

3.2. Assessment of the phylogenetic signal of single mt genes and subsets of genes

Maximum likelihood phylogenies were inferred from nucleotide sequence alignments of the complete set of mt genes (16 coding genes in total). The percentage of polymorphic sites varied amongst studied genes, ranging from 8.9% to 53% (Table 1). We assessed the phylogenetic signal of single mt genes, which was compared with the supergene signal via Shimodaira–Hasegawa (SH) test (Fig. 2). These comparisons allowed us to determine the performance of single mt genes, and to determine the best combination of gene subsets with phylogenies similar to the supergene phylogeny. Twelve topologies inferred from single mt genes showed a significant reduction in log-likelihood (Ln*L*) and statistically different topologies from that shown in the supergene topology (Fig. 2). However, the other four genes (i.e. *rnl*, *nad5*, *cox1* and *nad2*), which were the longest mt genes, reproduced similar topologies to the supergene tree, with much more subtle decreases in Ln*L* relative to the supergene phylogeny (Fig. 2). Visual inspection, coupled with statistical tests of single gene topologies, showed that the other mt genes provided poorly supported trees for two main reasons: (i) genes such as *atp9*, *cob*, *cox2* and *rns* could not resolve distant taxa such as *Gigaspora* spp. and *Glomus cerebriforme* from *Rhizophagus* spp.; (ii) *nad4L*, *nad6*, and *atp8* genes provided low resolution for resolving *Rhizophagus* sp. isolates from other *Rhizophagus irregularis*, which has been showed to be divergent (e.g. topologies inferred from *cob* and *nad4L* are demonstrated in Fig. 3). Furthermore, we evaluated the minimum number of concatenated mt genes required to statistically reproduce a topology similar to that of the supergene using ML. A SH test of the combination of 'best-performing' genes revealed low decreases in log-likelihood scores (Fig. 2). Phylogenies inferred from combinations of genes containing *cox1* with *nad2* or *rnl*, provided topologies that are statistically identical to the supergene topology (Fig. 3), with the smallest decreases in Ln*L* (Fig. 2).

Here we demonstrate that choosing a single mt gene in phylogenetic analysis may not reflect the phylogeny of the complete set of mt coding genes. Some studies have shown that phylogenies from combinations of all mt genes or from complete mitogenomes represent the highest phylogenetic performance and more robust results than those produced by single genes and gene subsets (Duchene et al., 2011; Havird and Santos, 2014). These studies

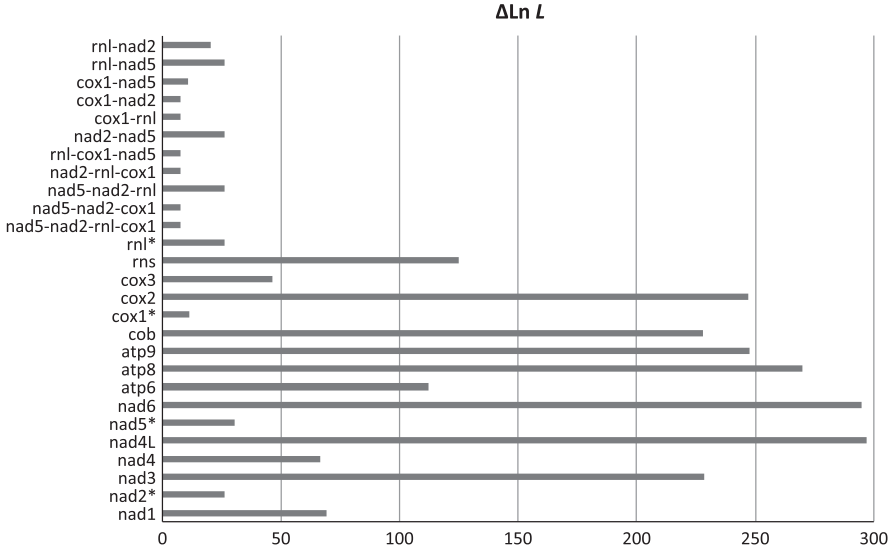

Fig. 2. Difference in log-likelihood measured via SH test by comparing phylogenetic topologies inferred from single mt genes relative to that of the "supergene" set. Difference in Ln*L* compared to the supergene phylogeny for all 16 mt genes (*y*-axis) has been shown on the *x*-axis as Δ Ln*L*. The four best-performing genes (i.e., *cox1*, *rnl*, *nad5* and *nad2*) are indicated by ∗. Phylogenetic analyses were performed under ML and SH test implemented by RAxML locally.

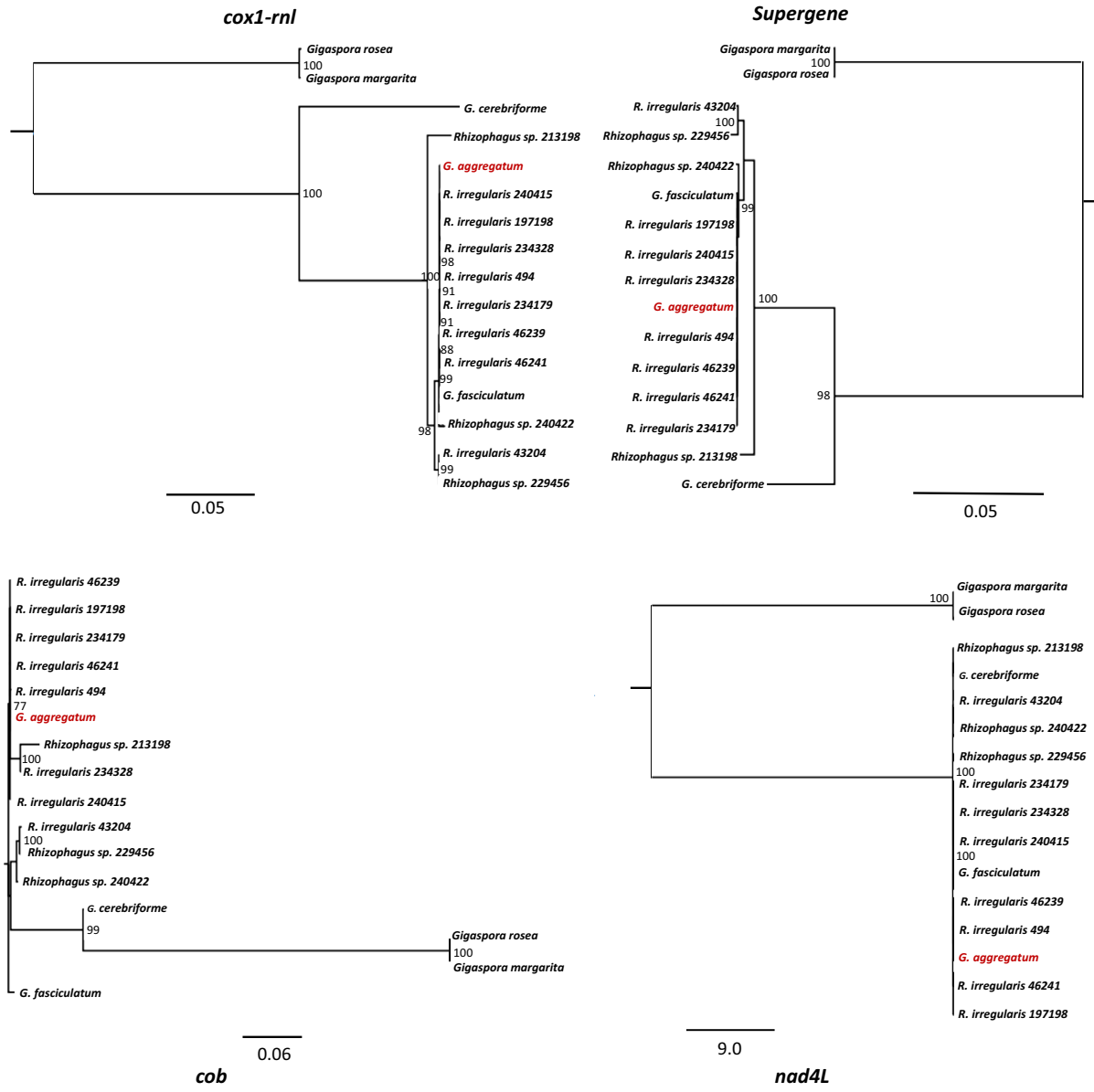

Fig. 3. Topologies inferred from supergene set and concatenated set of *rnl* and *cox1* revealing their high concordance in addition to topologies inferred from *nad4L* and *cob* as an example of individual genes with significant inconcordance to supergene topology. (A) The two phylogenies are significantly congruent based on statistical analyses of Shimodaira–Hasegawa (SH) with a difference of 7.6 in their Ln*L* values. Combination of *cox1* and *nad2* also showed a statistically congruent topology, which is not repeated here. The supergene set consists of a concatenation of all mt coding genes (i.e. 16 genes). *rnl*, *cox1* are the two largest mt genes. *G. aggregatum* is colored as red to highlight its position within the *Rhizophagus* clade. Numbers at nodes represent bootstrap support values. Phylogenies were inferred using DNA sequences and maximum likelihood (scale bars indicate replacements per site). (B) Topologies inferred by *nad4L* and *cob* DNA sequences showing significant decreases in Ln*L* values compared with supergene topology (ΔLn*L* of 294.6 and 228.1 respectively). *Cob* is not able to resolve distant taxa such as *Gigaspora* spp. and *Glomus cerebriforme* from *Rhizophagus* spp. while *nad4L* possesses low resolution for resolving *Rhizophagus* sp. isolates from other *Rhizophagus irregularis*. (For interpretation of the references to color in this figure legend, the reader is referred to the web version of this article.)

identified the most informative mt regions (genes) and evaluated the minimum amount of data required to infer phylogenies that were similar to supergene or complete mtDNA topologies. Therefore, the most informative mt genes or regions might vary among taxonomic groups and organisms (Duchene et al., 2011; Havird and Santos, 2014).

Mt genes *rnl* and *cox1* have previously been used independently to infer phylogenies among taxa of the Glomeromycota (Borriello et al., 2014; Borstler et al., 2008; Raab et al., 2005). Our study demonstrates that phylogenetic analysis that combines *cox1* and either *rnl* or *nad2* performs better than analysis on individual genes, not only considering the performed phylogenetic analyses, but also the evolutionary features of each individual gene. There are certain evolutionary aspects of *rnl* and *cox1* that need to be considered prior to their use in phylogenetic analyses of either organelles or organisms. For example, it is known that *rnl* is able to carry inserts and introns in variable regions that are not excised at the RNA level (Raab et al., 2005). Thus, it is often not easy to align mitochondrial rDNA sequences across species, due to introns, insertions, and the loss of domains. There is still no reliable method for inferring precise ends of the *rnl* gene, as the sequences of both terminal regions are highly variable. The only method for precise annotation is RNA analysis (Lang et al., 1987; Nadimi et al., 2012). However, most of the available *rnl* sequences in public databases are not annotated precisely. Therefore, *rnl* can be useful for short distance species phylogenies, but would be problematic for

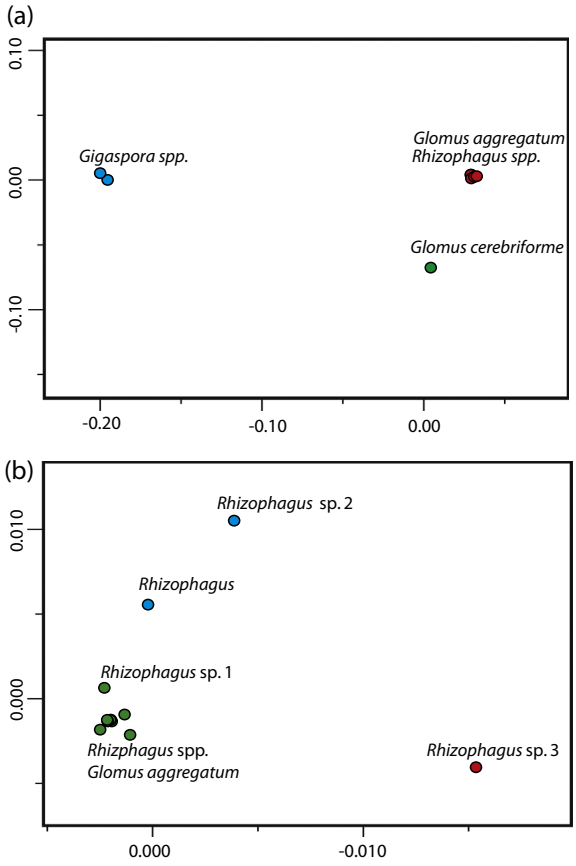

Fig. 4. PCoA plot based on the distance matrix obtained from mitochondrial genomic alignments (a) using all 16 mtDNAs examined in this study. *Gigaspora* spp. (*Gi. rosea*, and *Gi. margarita*) and *Glomus cerebriforme* are distinguished from the *Rhizophagus* spp. and *Glomus aggregatum* isolates. Two groups inferred by clustering analysis are shown in colors, (b) using 12 isolates of *Rhizophagus* spp. and *G. aggregatum*. The three groups inferred by clustering analysis are shown in different colors. (For interpretation of the references to color in this figure legend, the reader is referred to the web version of this article.)

phylogenies that attempt to resolve among fungal clades or deeper levels. There are also several reports regarding the evolutionary history and structure of *cox1*, which hampered the use of this gene for annotation, phylogenetic analyses and barcoding. For example, Nadimi et al. (2012) reported the occurrence of a group I intron-mediated trans-splicing in *cox1* of *Gigaspora rosea* that has been previously described in several other organisms (Burger et al., 2009; Grewe et al., 2009; Hecht et al., 2011; Nadimi et al., 2012; Pombert and Keeling, 2010). Frequent horizontal gene transfer within the introns of this gene, which has been reported in the literature (Beaudet et al., 2013a; Lang and Hijri, 2009), may also complicate the sequencing and assembly of this region, as well as downstream phylogenetic analyses. In the case of *cox1*, its annotation is easier compared with *rnl* gene. This is mainly due to the high number of publically available annotated *cox1* sequences which facilitates nucleotide sequence comparison and annotation of newly sequenced *cox1* genes. The above-mentioned findings limit the usefulness of individual *rnl* and *cox1* genes for phylogenetic analyses of AMF. The mentioned points are also important to be considered for successful annotation and phylogenetic analyses. Combinations of multiple genes (e.g., different combinations of *cox1*, *rnl* and *nad2*) may help to overcome these drawbacks.

3.3. Assessment of the relationship between isol

To further evaluate the relationships between all 16 isolates used in this study, we performed a principal coor e analysis (PCoA) based on the distance matrix obtained from mitochondrial nucleotide alignments (Fig. 4). The PCoA plot shows that all *Rhizophagus* spp. isolates and *G. aggregatum* group together. Of the other three isolates, *G. cerebriforme* is apart, while both *Gigaspora spp.* cluster more closely together. Both partitioning methods used (k-means and k-medoids) created two groups, corresponding to the two orders (Glomerales and Diversisporales) used in the study. When inferring three groups instead of two on the plot, only *G. cerebriforme* separates from the Glomerales group to form the third group. To further assess the cluster of *Rhizophagus* isolates, another principal coordinate analysis (PCoA) was computed, excluding both *Gigaspora* species and *G. cerebriforme* (Fig. 4). Both partitioning methods inferred three groups, the first including solely *Rhizophagus* sp. DAOM213198, the second including *R. irregularis* MUCL43204 and *Rhizophagus* sp. DAOM229456, and the third including the remaining nine *Rhizophagus* isolates and *G. aggregatum*. One *Rhizophagus* sp. isolate, DAOM240422, clustered with the other nine *Rhizophagus* isolates, but with a weaker similarity (Fig. 4). These results support the *G. cerebriforme* isolate as genetically distant from all *Rhizophagus* isolates and from the *G. aggregatum* isolate used in this study. As discussed above,

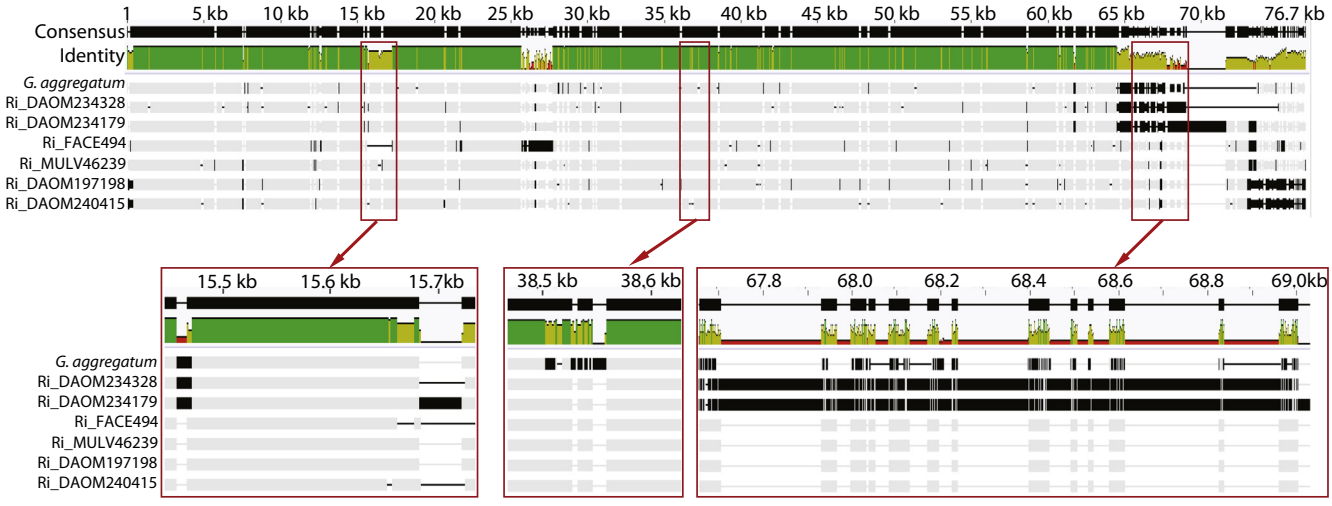

Fig. 5. Complete mtDNA alignment of *R. irregularis* isolates and *G. aggregatum* showing sequence variations in intergenic regions, while coding genes are almost identical.

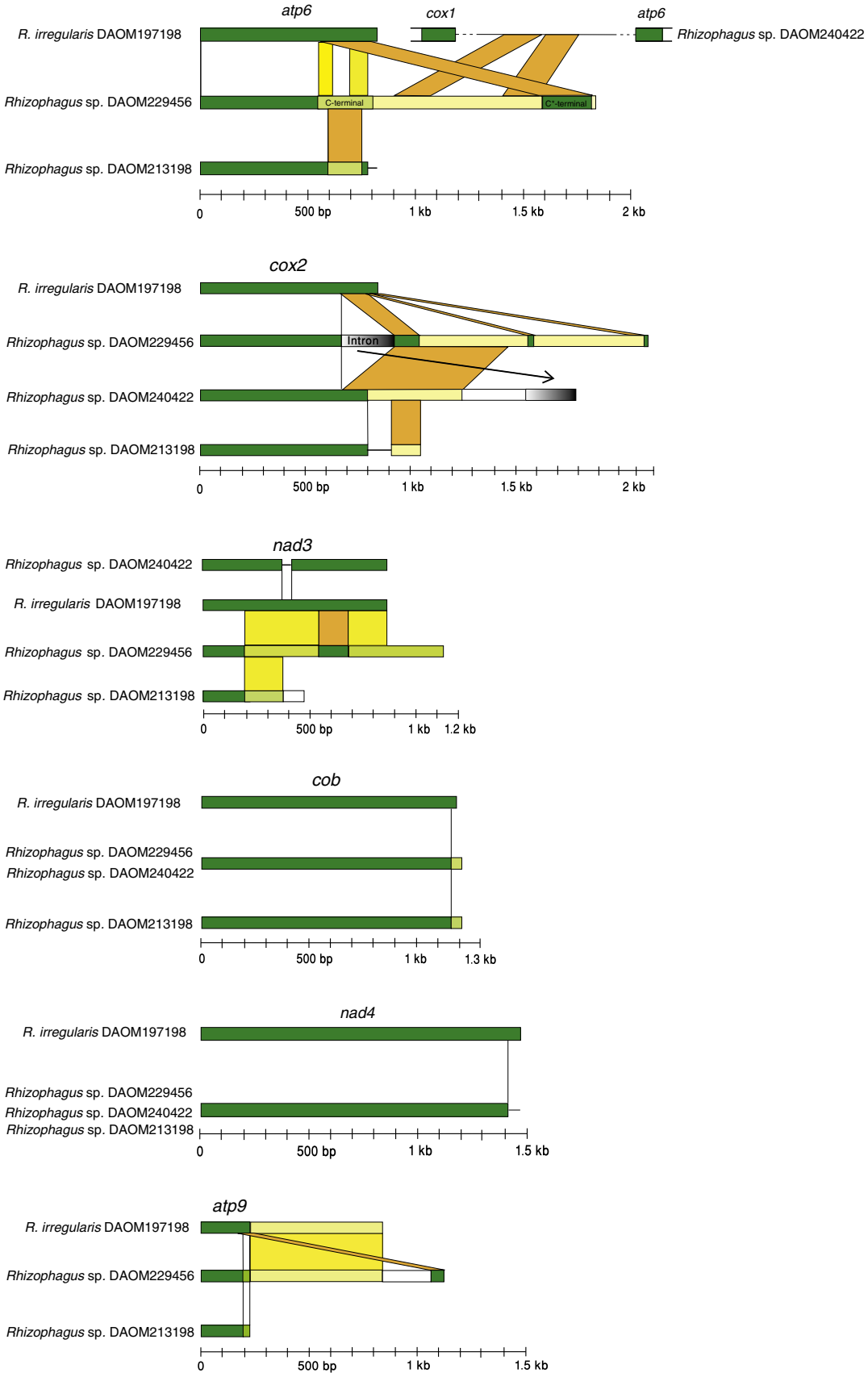

Fig. 6. Linear genome representations of some mt genes, harboring the relative recombinations within the *Rhizophagus* sp. complex to compare with *R. irregularis*. Corresponding genes (*atp6*, *cox2*, *nad3*, *cob*, *nad4* and *atp9*) among *R. irregularis* DAOM197198 and *Rhizophagus* sp. DAOM240422, DAOM213198 and DAOM229456 are linearized and compared using projections. Projections in yellow represent nucleotide identity at more than 90%, while projections in orange illustrate the identity of more that 90% at the amino acid level. Projections with no color were used to facilitate detection of related regions. The intron formed in *Rhizophagus* sp. DAOM229456 is boxed in gray, which is transferred to the intergenic region after *cox2* in *Rhizophagus* sp. DAOM240422. Nucleotide and amino acid identity comparisons were performed via blastn and tblastx among the studied AMF isolates. (For interpretation of the references to color in this figure legend, the reader is referred to the web version of this article.)

spore morphology and phosphate transporter phylogeny are able to marginally discriminate between *G. aggregatum* from *Rhizophagus* isolates. However, our analysis based on the complete mt genome shows that other *Rhizophagus* isolates, such as *R. irregularis* MUCL43204 and *Rhizophagus* sp. DAOM213198/DAOM299456 are genetically more distant from the other nine *R. irregularis* isolates than is *G. aggregatum*. This evidence supports the position of *G. aggregatum* within the *Rhizophagus irregularis* 'species complex'.

3.4. Unraveling the Rhizophagus irregularis complex

Comparative mitogenomics analysis of *R. irregularis* isolates (Fig. 5) and *Rhizophagus* spp. reveals a high level of homogeneity within the coding sequences, while intronic and intergenic regions showed substantial variable regions, which is consistent with the rate of evolutionary constraint based on the functions of different mtDNA regions. However, comparative analyses using ML and PCoA of coding regions suggest the occurrence of unorthodox recombinations (Fig. 6) among some *Rhizophagus* spp. isolates (DAOM229456, DAOM240422 and DAOM213198) with uncertain classification, grouping them apart from other known *R. irregularis* isolates. Genetic recombinations may have taken place at different points during the evolutionary history of the different isolates or of a recent common ancestor, although horizontal gene transfer of recombined regions is also a possibility. A shared common ancestor seems to be the most parsimonious and plausible, due to similar signatures observed in recombined regions (Fig. 6). Mt genes *atp6*, *cox2*, *nad3*, *cob*, *nad4* and *atp9* are examples of these recombined mt genes within *Rhizophagus* spp. (Beaudet et al., 2013a, 2013b).

Comparative analyses of the intergenic regions of *Rhizophagus* spp. showed relatively higher levels of similarity in up- and down-stream sequences of coding genes compared to other intergenic regions. Up- and down-stream sequences of coding genes include 5′ and 3′ extensions of genes (known as 5′ and 3′ untranslated regions), which are transcribed but not translated. The conservation of such regions is due to their function, therefore resulting in a slower rate of evolution relative to non-functional regions. Consequently, comparative analyses of multiple sequence alignments of complete mtDNAs grouped *Rhizophagus* spp. isolates among the *Rhizophagus irregularis* species, which we suggest to be considered as a species complex (e.g. *Rhizophagus irregularis* complex).

4. Conclusion

We implemented the existing mtDNA dataset with two newly completed and annotated mt genomes. Our mitogenomic comparative analysis among several AMF species and isolates allowed us to assess the phylogenetic signals of individual mt genes in comparison to the supergene set. A statistical SH test revealed that the evolutionary signal differed significantly between single mt genes, subsets of genes, and the supergene in the Glomeromycota. The combination of *cox1* with either *rnl* or *nad2* genes is a promising subset of mt genes that could be useful in inferring phylogenies within Glomeromycota. However, implementation of the mtDNA dataset with members of other families and genera is needed to cover the diversity of the Glomeromycota phylum and to infer robust phylogenies. Further studies on the comparison and potential combination of mt gene subsets, supergenes, and nuclear ribosomal rRNA genes could provide a higher phylogenetic resolution, and may help to discriminate between closely related members of the Glomeromycota.

Acknowledgments

This work was supported by the Natural Sciences and Engineering Research Council of Canada (Discovery grant 328098-2012 to M.H.). Our thanks to Dr. B.F. Lang for bioinformatics assistance and access to an automated organelle genome annotation software, to Dr. Y. Dalpé for kindly providing fungal material, Dr. S. Joly for assistance in phylogenetic and statistical analyses, and Dr. T. Bell for commenting on the manuscript and English editing.

Appendix A. Supplementary material

Supplementary data associated with this article can be found, in the online version, at http://dx.doi.org/10.1016/j.ympev.2016.01.009.

References

Angelard, C., Colard, A., Niculita-Hirzel, H., Croll, D., Sanders, I.R., 2010. Segregation in a mycorrhizal fungus alters rice growth and symbiosis-specific gene transcription. Curr. Biol. 20, 1216–1221.
Avise, J.C., 1994. Molecular Markers, Natural History and Evolution. Chapman & Hall, New York.
Azcón-Aguilar, C., Barea, J.M., 1997. Arbuscular mycorrhizas and biological control of soil-borne plant pathogens – an overview of the mechanisms involved. Mycorrhiza 6, 457–464.
Beaudet, D., Nadimi, M., Iffis, B., Hijri, M., 2013a. Rapid mitochondrial genome evolution through invasion of mobile elements in two closely related species of arbuscular mycorrhizal fungi. PLoS One 8, e60768.
Beaudet, D., Terrat, Y., Halary, S., de la Providencia, I.E., Hijri, M., 2013b. Mitochondrial genome rearrangements in glomus species triggered by homologous recombination between distinct mtDNA haplotypes. Genome Biol. Evol. 5, 1628–1643.
Beaudet, D., de la Providencia, I.E., Labridy, M., Roy-Bolduc, A., Daubois, L., Hijri, M., 2015. Intra-isolate mitochondrial genetic polymorphism and gene variants co-expression in arbuscular mycorrhizal fungi. Genome Biol. Evol. 7 (1), 218–227.
Bécard, G., Fortin, J.A., 1988. Early events of vesicular–arbuscular mycorrhiza formation on Ri T-DNA transformed roots. New Phytol. 108, 211–218.
Bianciotto, V., Lumini, E., Bonfante, P., Vandamme, P., 2003. '*Candidatus glomeribacter gigasporarum*' gen. nov., sp. nov., an endosymbiont of arbuscular mycorrhizal fungi. Int. J. Syst. Evol. Microbiol. 53, 121–124.
Boon, E., Zimmerman, E., Lang, B.F., Hijri, M., 2010. Intra-isolate genome variation in arbuscular mycorrhizal fungi persists in the transcriptome. J. Evol. Biol. 23, 1519–1527.
Boon, E., Zimmerman, E., St-Arnaud, M., Hijri, M., 2013. Allelic differences among sister spores suggest genetic drift in an arbuscular mycorrhizal fungus. PLoS One 8, e83301.
Boon, E., Halary, S., Bapteste, E., Hijri, M., 2015. Studying genome heterogeneity within the arbuscular mycorrhizal fungal cytoplasm. Genome Biol. Evol. 7 (2), 505–521.
Borriello, R., Bianciotto, V., Orgiazzi, A., Lumini, E., Bergero, R., 2014. Sequencing and comparison of the mitochondrial COI gene from isolates of Arbuscular Mycorrhizal Fungi belonging to Gigasporaceae and Glomeraceae families. Mol. Phylogenet. Evol. 75, 1–10.
Borstler, B., Raab, P.A., Thiery, O., Morton, J.B., Redecker, D., 2008. Genetic diversity of the arbuscular mycorrhizal fungus *Glomus intraradices* as determined by mitochondrial large subunit rRNA gene sequences is considerably higher than previously expected. New Phytol. 180, 452–465.
Bruns, T.D., Szaro, T.M., Gardes, M., Cullings, K.W., Pan, J.J., Taylor, D.L., Horton, T.R., Kretzer, A., Garbelotto, M., Li, Y., 1998. A sequence database for the identification of ectomycorrhizal Basidiomycetes by phylogenetic analysis. Mol. Ecol. 7, 257–272.
Burger, G., Yan, Y., Javadi, P., Lang, B.F., 2009. Group I-intron trans-splicing and mRNA editing in the mitochondria of placozoan animals. Trends Genet. 25, 381–386.
Charif, D., Lobry, J., 2007. SeqinR 1.0-2: a contributed package to the R project for statistical computing devoted to biological sequences retrieval and analysis. In: Bastolla, U., Porto, M., Roman, H.E., Vendruscolo, M. (Eds.), Structural Approaches to Sequence Evolution. Springer, Berlin, Heidelberg, pp. 207–232.
de la Providencia, I.E., Nadimi, M., Beaudet, D., Morales, G.R., Hijri, M., 2013. Detection of a transient mitochondrial DNA heteroplasmy in the progeny of crossed genetically divergent isolates of arbuscular mycorrhizal fungi. New Phytol. 200, 211–221.
Duchene, S., Archer, F.I., Vilstrup, J., Caballero, S., Morin, P.A., 2011. Mitogenome phylogenetics: the impact of using single regions and partitioning schemes on topology, substitution rate and divergence time estimation. PLoS One 6, e27138.
Edgar, R.C., 2004. MUSCLE: multiple sequence alignment with high accuracy and high throughput. Nucleic Acids Res. 32, 1792–1797.

Fenn, J.D., Song, H., Cameron, S.L., Whiting, M.F., 2008. A preliminary mitochondrial genome phylogeny of Orthoptera (Insecta) and approaches to maximizing phylogenetic signal found within mitochondrial genome data. Mol. Phylogenet. Evol. 49, 59–68.

Formey, D., Moles, M., Haouy, A., Savelli, B., Bouchez, O., Becard, G., Roux, C., 2012. Comparative analysis of mitochondrial genomes of *Rhizophagus irregularis* – syn. *Glomus irregulare* – reveals a polymorphism induced by variability generating elements. New Phytol. 196, 1217–1227.

Garcia-Garrido, J.M., Ocampo, J.A., 2002. Regulation of the plant defence response in arbuscular mycorrhizal symbiosis. J. Exp. Bot. 53, 1377–1386.

Grewe, F., Viehoever, P., Weisshaar, B., Knoop, V., 2009. A trans-splicing group I intron and tRNA-hyperediting in the mitochondrial genome of the lycophyte *Isoetes engelmannii*. Nucleic Acids Res. 37, 5093–5104.

Halary, S., Malik, S.-B., Lildhar, L., Slamovits, C.H., Hijri, M., Corradi, N., 2011. Conserved meiotic machinery in *Glomus* spp., a putatively ancient asexual fungal lineage. Genome Biol. Evol. 3, 950–958.

Halary, S., Daubois, L., Terrat, Y., Ellenberger, S., Wostemeyer, J., Hijri, M., 2013. Mating type gene homologues and putative sex pheromone-sensing pathway in arbuscular mycorrhizal fungi, a presumably asexual plant root symbiont. PLoS One 8, e80729.

Havird, J.C., Santos, S.R., 2014. Performance of single and concatenated sets of mitochondrial genes at inferring metazoan relationships relative to full mitogenome data. PLoS One 9, e84080.

Hebert, P.D., Ratnasingham, S., deWaard, J.R., 2003. Barcoding animal life: cytochrome c oxidase subunit 1 divergences among closely related species. Proc. Biol. Sci./Roy. Soc. 270 (Suppl. 1), S96–S99.

Hecht, J., Grewe, F., Knoop, V., 2011. Extreme RNA editing in coding islands and abundant microsatellites in repeat sequences of *Selaginella moellendorffii* mitochondria: the root of frequent plant mtDNA recombination in early tracheophytes. Genome Biol. Evol. 3, 344–358.

Hennig, C., 2010. fpc: Flexible Procedures for Clustering. R Package Version 2, pp. 0–3.

Hijri, M., Sanders, I.R., 2005. Low gene copy number shows that arbuscular mycorrhizal fungi inherit genetically different nuclei. Nature 433, 160–163.

Hijri, M., Redecker, D., Petetot, J.A.M.-C., Voigt, K., Wöstemeyer, J., Sanders, I.R., 2002. Identification and isolation of two *Ascomycete* fungi from spores of the arbuscular mycorrhizal fungus *Scutellospora castanea*. Appl. Environ. Microbiol. 68, 4567–4573.

Hildebrandt, U., Kaldorf, M., Bothe, H., 1999. The zinc violet and its colonization by arbuscular mycorrhizal fungi. J. Plant Physiol. 154, 709–717.

Iffis, B., St-Arnaud, M., Hijri, M., 2014. Bacteria associated with arbuscular mycorrhizal fungi within roots of plants growing in a soil highly contaminated with aliphatic and aromatic petroleum hydrocarbons. FEMS Microbiol. Lett. 358, 44–54.

Ismail, Y., Hijri, M., 2012. Arbuscular mycorrhisation with *Glomus irregulare* induces expression of potato PR homologues genes in response to infection by *Fusarium sambucinum*. Funct. Plant Biol. 39, 236–245.

Ismail, Y., McCormick, S., Hijri, M., 2011. A fungal symbiont of plant-roots modulates mycotoxin gene expression in the pathogen *Fusarium sambucinum*. PLoS One 6, e17990.

Kuhn, G., Hijri, M., Sanders, I.R., 2001. Evidence for the evolution of multiple genomes in arbuscular mycorrhizal fungi. Nature 414, 745–748.

Lang, B.F., Hijri, M., 2009. The complete *Glomus intraradices* mitochondrial genome sequence – a milestone in mycorrhizal research. New Phytol. 183, 3–6.

Lang, B.F., Cedergren, R., Gray, M.W., 1987. The mitochondrial genome of the fission yeast, *Schizosaccharomyces pombe*. Sequence of the large-subunit ribosomal RNA gene, comparison of potential secondary structure in fungal mitochondrial large-subunit rRNAs and evolutionary considerations. Eur. J. Biochem. 169, 527–537.

Lecomte, J., St-Arnaud, M., Hijri, M., 2011. Isolation and identification of soil bacteria growing at the expense of arbuscular mycorrhizal fungi. FEMS Microbiol. Lett. 317, 43–51.

Lee, J., Young, J.P., 2009. The mitochondrial genome sequence of the arbuscular mycorrhizal fungus *Glomus intraradices* isolate 494 and implications for the phylogenetic placement of *Glomus*. New Phytol. 183, 200–211.

Librado, P., Rozas, J., 2009. DnaSP v5: a software for comprehensive analysis of DNA polymorphism data. Bioinformatics 25, 1451–1452.

Lohse, M., Drechsel, O., Kahlau, S., Bock, R., 2013. OrganellarGenomeDRAW – a suite of tools for generating physical maps of plastid and mitochondrial genomes and visualizing expression data sets. Nucleic Acids Res. 41, W575–W581.

Marleau, J., Dalpe, Y., St-Arnaud, M., Hijri, M., 2011. Spore development and nuclear inheritance in arbuscular mycorrhizal fungi. BMC Evol. Biol. 11, 51.

Miller, M.A., Pfeiffer, W., Schwartz, T., 2010. Creating the CIPRES Science Gateway for inference of large phylogenetic trees. Gateway Computing Environments Workshop (GCE), 2010, pp. 1–8.

Nadimi, M., Beaudet, D., Forget, L., Hijri, M., Lang, B.F., 2012. Group I intron-mediated trans-splicing in mitochondria of *Gigaspora rosea* and a robust phylogenetic affiliation of arbuscular mycorrhizal fungi with Mortierellales. Mol. Biol. Evol. 29, 2199–2210.

Nadimi, M., Stefani, F.O.P., Hijri, M., 2015. The mitochondrial genome of the glomeromycete *Rhizophagus* sp. DAOM 213198 reveals an unusual organization consisting of two circular chromosomes. Genome Biol. Evol. 7 (1), 96–105.

Paradis, E., Claude, J., Strimmer, K., 2004. APE: analyses of phylogenetics and evolution in R language. Bioinformatics 20, 289–290.

Pawlowska, T.E., Taylor, J.W., 2004. Organization of genetic variation in individuals of arbuscular mycorrhizal fungi. Nature 427, 733–737.

Pelin, A., Pombert, J.F., Salvioli, A., Bonen, L., Bonfante, P., Corradi, N., 2012. The mitochondrial genome of the arbuscular mycorrhizal fungus *Gigaspora margarita* reveals two unsuspected trans-splicing events of group I introns. New Phytol. 194, 836–845.

Pombert, J.F., Keeling, P.J., 2010. The mitochondrial genome of the entomoparasitic green alga helicosporidium. PLoS One 5, e8954.

Raab, P.A., Brennwald, A., Redecker, D., 2005. Mitochondrial large ribosomal subunit sequences are homogeneous within isolates of *Glomus* (arbuscular mycorrhizal fungi, *Glomeromycota*). Mycol. Res. 109, 1315–1322.

Ratnasingham, S., Hebert, P.D., 2007. bold: The Barcode of Life Data System (http://www.barcodinglife.org). Molecular Ecology Notes 7, pp. 355–364.

Roe, A.D., Sperling, F.A., 2007. Patterns of evolution of mitochondrial cytochrome c oxidase I and II DNA and implications for DNA barcoding. Mol. Phylogenet. Evol. 44, 325–345.

Ropars, J., Corradi, N., 2015. Homokaryotic vs heterokaryotic mycelium in arbuscular mycorrhizal fungi: different techniques, different results? New Phytol. 208 (3), 638–641.

Schenck, N.C., Smith, G.S., 1982. Additional new and unreported species of mycorrhizal fungi (Endogonaceae) from Florida. Mycologia 77, 566–574.

Scheublin, T.R., Sanders, I.R., Keel, C., van der Meer, J.R., 2010. Characterisation of microbial communities colonising the hyphal surfaces of arbuscular mycorrhizal fungi. ISME J. 4, 752–763.

Schüssler, A., Walker, C., 2010. The Glomeromycota: A Species List with New Families and Genera. Edinburgh & Kew, UK: The Royal Botanic Garden; Munich, Germany: Botanische Staatssammlung Munich; OR, USA: Oregon State University. <http://schuessler.userweb.mwn.de/amphylo/Schuessler&Walker2010_Glomeromycota.pdf>.

Smith, S.E., Read, D.J., 2008. Mycorrhizal Symbiosis, third ed. Academic Press and Elsevier, London.

Sokolski, S., Dalpe, Y., Piche, Y., 2011. Phosphate transporter genes as reliable gene markers for the identification and discrimination of arbuscular mycorrhizal fungi in the genus glomus. Appl. Environ. Microbiol. 77, 1888–1891.

Stamatakis, A., Hoover, P., Rougemont, J., 2008. A rapid bootstrap algorithm for the RAxML Web servers. Syst. Biol. 57, 758–771.

Thiery, O., Borstler, B., Ineichen, K., Redecker, D., 2010. Evolutionary dynamics of introns and homing endonuclease ORFs in a region of the large subunit of the mitochondrial rRNA in *Glomus* species (arbuscular mycorrhizal fungi, *Glomeromycota*). Mol. Phylogenet. Evol. 55, 599–610.

Tisserant, E., Malbreil, M., Huang, S., Kuo, A., Kohler, A., Symeonidi, A., Balestrini, R., Charron, P., Formey, D., Geurts, R., Gianinazzi-Pearson, V., Gilbert, B., Hijri, M., Kaul, R., Krajinski, F., Lammers, P., Lapierre, D., Masclaux, F., Murat, C., Morin, E., Ndikumana, S., Pagni, M., Petitpierre, D., Requena, N., Rosikiewicz, P., Riley, R., Saito, K., San Clemente, H., Shapiro, H., van Tuinen, D., Bécard, G., Bonfante, P., Paszkowski, U., Shachar-Hill, Y., Young, J.P.W., Zhang, Z., Sanders, I.R., Henrissat, B., Rensing, S.A., Grigoriev, I.V., Bisseling, T., Corradi, N., Roux, C., Martin, F., 2013. Genome of an arbuscular mycorrhizal fungus provides insight into the oldest plant symbiosis. Proc. Natl. Acad. Sci. USA 110 (50), 20117–20122.

Zhang, X., Ren, B.H., Wu, S.L., Sun, Y.Q., Lin, G., Chen, B.D., 2014. Arbuscular mycorrhizal symbiosis influences arsenic accumulation and speciation in *Medicago truncatula* L. in arsenic-contaminated soil. Chemosphere 119C, 224–230.